Biochemical Amplification Waves in a One-Dimensional Microflow System

T. Kirner,* D. Steen,† J. S. McCaskill, and J. Ackermann

Fraunhofer-Gesellschaft, Schloss Birlinghoven, D-53754 Sankt Augustin, Germany

Received: September 27, 2001; In Final Form: January 5, 2002

A cooperatively coupled, isothermal biochemical amplification system has been investigated under flow conditions in a microstructured reactor. The experimental setup provides for continuous amplification and on line detection of the reaction products in space and time. Spatially resolved fluorescence spectroscopy with an intercalating dye was used for detection of the double stranded DNA products. Biochemical amplification was observed under a wide range of flow rates. The total rate of amplification resulted from an interplay between the amplification of the biochemical system and a loss term produced by the flow. For flow rates above a critical value, the system was diluted out and the amplification reaction brought to a halt in the reactor. Homogeneous growth throughout the reactor was observed at intermediate flow rates. At low pump rates, additional biochemical amplification started at various locations. We interpret the spatially homogeneous growth at low concentration and the local growth at high concentration to result from two different amplification phases because of noncooperative and cooperative amplification mechanisms, respectively. The consequences for long-term evolutionary experiments as well as for complex pattern formation are discussed.

1. Introduction

Molecules such as DNA or RNA are carriers of information. The amount of information (sequence length) which can be stably reproduced through simple independent replicators has a natural limit which is inversely proportional to the monomer error rate during replication.[1] Catalytic coupling between molecules is necessary for chemical evolution to reach higher mechanistic and functional complexity.[2−8] However, in evolutionary processes, hetero-catalytic or cooperative coupling can be exploited by emerging parasites.[9,10] To avoid such exploitation, compartmentation was deemed necessary.[2,9−11] An alternative mechanism for stabilizing the evolution of cooperativity is to use the pattern-forming capabilities of continuous systems.[12−16]

The first experiments on spatially resolved in vitro evolution were performed with the amplification of RNA using the in vitro Qβ replicase system in translucent polyethylene capillaries.[17,18] Replication waves with relatively sharp wave fronts and constant velocity between evolutionary transitions were observed in these experiments. A greater variety of self-organization phenomena is possible if an amplification system can be kept in a dissipative nonequilibrium state indefinitely. This is possible in an open reactor operating under flow conditions.[19] The system must be fed with resources without spatial mixing, and products must be removed. Because of the high costs of enzymes and oligonucleotides, it is useful to reduce the reaction volume to a minimum. Microstructurable materials such as silicon, glass, or polymers allow the miniaturization of reaction vessels down to the micrometer range.[20,21]

In population genetics theory, cooperative or altruistic alleles can survive in structured populations (cooperation generally involves costs for the individual, because of the generic existence of variants able to exploit the positive characteristics of the cooperator). One example is the island model of Wright,[22,23] as investigated by Kimura and Aoki.[24,25] With dividing compartments, Szathmáry made this effect well-known as the stochastic corrector model.[26] To investigate the evolution of cooperation between simple replicators, a trans-cooperatively coupled biochemical system called CATCH (cooperative amplification of templates by cross hybridization) was established.[27] This system is based on the 3SR (self-sustained sequence replication) reaction,[28,29,30] also known as NASBA (nucleic acid sequence-based amplification).[31,32] A theoretical analysis of the CATCH reaction showed its ability to form patterns in a spatially resolved flow reactor.[33]

Serial transfer experiments have shown that the CATCH system will evolve under certain conditions to a tri-cyclic system.[34] In this system, two RNA-Z-like hairpins[35,36] amplify independently. The species have complementary loop sequences, and the amplification includes concentration-dependent phases of noncooperative and cooperative amplification. Although space plays an important role in the evolution of cooperativity, spatially resolved experiments have never previously been done with in vitro molecular systems under flow conditions. We chose the tri-cyclic CATCH system to study the usefulness of spatially resolved microstructured flow reactors for biochemical amplification experiments.

The following work focuses on two main aspects. First, we study the influence of flow on the amplification. In this part, we answer the following questions: Can the reaction be started under flow conditions in a microstructured reactor and the amplification sustained over a long time frame? Is a critical flow rate observable for the amplification? How does the system react to varying flow rates, and how is the amplification rate influenced? The second part of the work deals with the influence of spatial resolution on the experiments. Is it possible to observe more complex behavior than homogeneous growth? Can information be gained from the spatial resolution about the kinetics of amplification inside the reactor? Is it possible to observe complex pattern formation in such reactors?

* To whom correspondence should be addressed. E-mail: thomas.kirner@gmd.de. Fax: +49-2241-141511.

† Institute for Molecular Biotechnology, Beutenbergstr. 11, D-07745 Jena, Germany. Present address: BioLitec AG, Winzerlaer Str. 2a, D-07745 Jena, Germany.

10.1021/jp013633o CCC: $22.00
Published on Web 04/06/2002

2. Experimental Section

2.1. Biochemical System. The tri-cyclic CATCH system consists of three interconnected amplification cycles. Two cycles amplify two different DNA strands called DNA_1 and DNA_2 according to a RNA-Z like mechanism. The third cooperative cycle starts by hybridizing two complementary regions of DNA_1 and DNA_2. DNA_1 serves as a primer for DNA_2 and vice versa. In the RNA-Z mechanism, the amplification of a given species is realized with only one primer and an internal RNA-polymerase promoter sequence.[35] The otherwise obligatory second primer is replaced by the intramolecular hybridization at the 3′ end. RNA−Z amplification takes place preferentially at very low concentrations, where the intermolecular DNA_1−DNA_2 binding reaction necessary for the cooperative mechanism[27] is negligible, because the concentrations of the two template partners have not reached the binding constant (in the nM range).[37] If the concentration exceeds the binding constant, the two amplification cycles are coupled trans-cooperatively through these single-stranded DNAs. It is then more efficient for the template to be amplified via the cooperative cycle. The product of the DNA_1−DNA_2 hybridization at the 3′ ends is completed by a reverse transcriptase (HIV-1-RT) to form a double-stranded DNA. This double stranded DNA has two promoter sequences for a DNA dependent RNA-polymerase (T7-RNA-Pol). The two promoters are inversely oriented on either side of the hybridization region. Starting at these promoter sequences, multiple copies of two different RNA strands are produced. By hybridization of two matching DNA primers followed by reverse transcription, the two RNA copies yield the species DNA_1 and DNA_2, respectively. For a detailed description of the system, we refer to refs 34 and 37. The following basic reaction mixture was used:

Primer P1 (5′-CCTCTGCAGACTACTATTAA-3′) 2 μM

Primer P2 (5′-CCTGAATTCTTGCTGTGACG-3′) 2 μM

40 mM Tris-HCl pH 8.1, 5 mM dithiotreitol, 2 mM spermidin (Sigma, Deisenhofen, Germany), 30 mM $MgCl_2$, 10 mM KCl, 1 mM dNTPs (C, G, A, T) and 2 mM rNTPs (C, G, A, U) (Pharmacia, Freiburg, Germany), 0.4 μg/μL BSA (Bovine Serum Albumin, free of nucleases, Roth, Karlsruhe, Germany), 3 μM TO-PRO-1 (Molecular Probes, Eugene, OR),[38] 2 U/μL His-tagged HIV-1-RT, 0.8 U/μL T7-RNA-Polymerase, 0.16 U/μL *E. coli* RNaseH (MBI Fermentas, Lithuania). Optionally, the two templates

DNA_1 (71 bases, 5′-CCTCTGCAGACTACTATTAC-*ATAATACGACTCGCTATA***GAGATTTTTATT-TATGAATTAAATAAATATCCC**-3′)

and

DNA_2 (75 bases, 5′-CCTGAATTCTTGCTGTGACG-*TTATTTAATACGACTCAC***TATAGGGATATT-TATTTAATTCATAAATAAAAATCTC**-3′)

were added to the solution at a concentration of 5−10 nM. The primer regions of the templates are underlined, the T7-promoter regions are italicized, and the hybridization regions, DB and DB′, are printed in bold face. Oligonucleotides were purchased from MWG Biotech (Ebersberg, Germany) and purified using high performance liquid chromatography (HPLC). All standard chemicals were reagent grade and were purchased from Sigma (Deisenhofen, Germany). HIV-1-RT and T7 RNAP both fused to a 6-Histidine tag were produced from recombinant *E. coli* strains and purified according to Le Grice et al.[39] and Ellinger and Ehricht,[40] respectively.

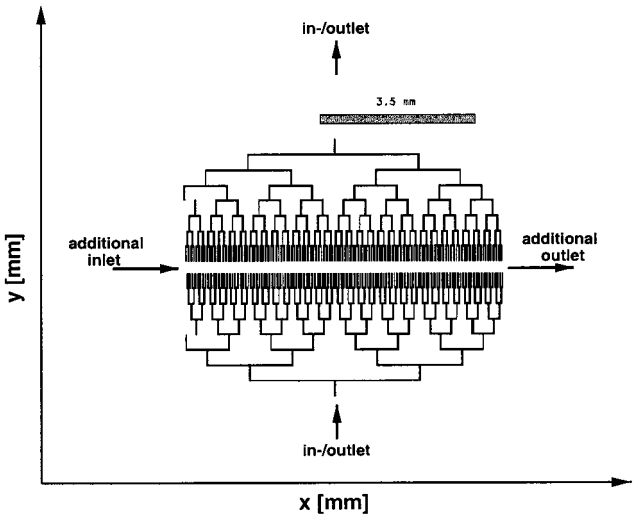

Figure 1. Sketch of the microstructured flow reactor. The bifurcation structure is used for homogeneous in- and outflow. Between these two bifurcation structures lies the reaction chamber. Additional inlets and outlets are attached laterally to the reaction chamber.

The reaction temperature was 42 ± 0.1 °C in all experiments. To reduce interactions of the polynucleotides and the proteins to surfaces, Solution Q (Qiagen, Hilden, Germany) was added to each reaction solution. The intercalating dye TO-PRO-1 has an excitation maximum at 514 nm and an emission maximum at 531 nm and was used for spatially monitoring amplification by laser-induced fluorescence (see below).

2.2. Microflow Reactor. To observe concentration waves and amplification of in vitro biochemical systems, a variety of microstructured reactors were developed.[41−44] One of these reactors was used in the experiments discussed in this paper (see Figure 1). The reactor was manufactured by wet chemical etching of silicon. The structure was then sealed by bonding Pyrex glass to the silicon.[41,43] Inlets and outlets were ultrasonically drilled through the glass layer to connect the fluidics to external pumps (SP200 Series, World Precision Instruments, Inc.). Polyethylene capillaries (NeoLab,Heidelberg, Germany, inner diameter 0.4 mm) were positioned using small plastic supports and glued to these holes as connecting tubing.

The structure shown in Figure 1 consists of two bifurcation structures to create uniform cross-flow, one for the inflow of reactants and one for the outflow of products with the elongated reaction chamber between them. The reaction chamber is quasi-one-dimensional. Its dimensions are 6 cm orthogonal to the flow and 60−80 μm deep. The anisotropic etching process gives a trapezoidal profile with an actual width of approximately 345 μm at the top and 225 μm at the bottom. The flow is transverse to the long axis of the reactor. Along the direction of the flow, diffusive mixing is calculated to take place below the time scale of replication in about 100 s (see below). The reaction chamber has a volume of 1.4 μL and for pump rates on the order of 1 μL/min, and the residence time is comparable to the time scale of diffusive mixing.

Homogeneous influx and outflux are realized along the full length of the reactor using the bifurcation structures. A total of 1024 channels were connected on each side of the chamber to attain this. To prevent back-propagation of amplification into the inlet structure, the flow rate in these channels had to be

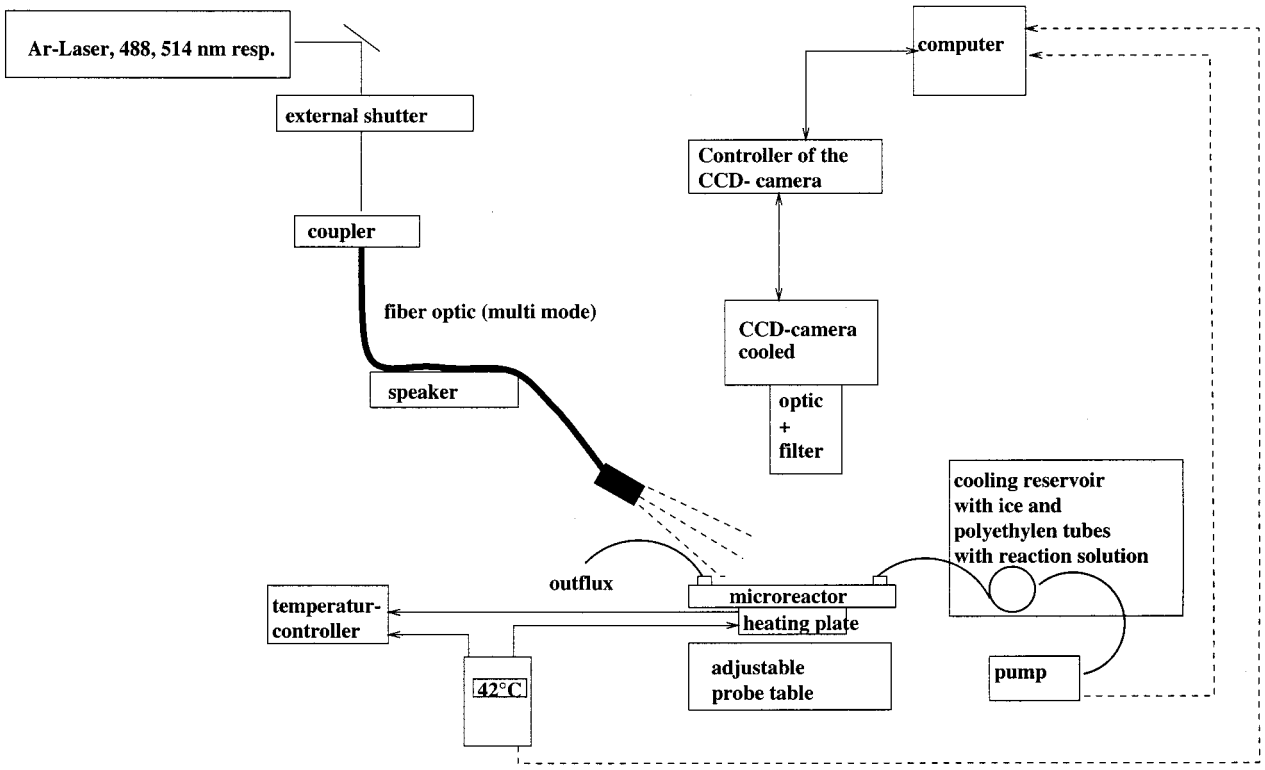

Figure 2. Argon-ion laser is used as light source. The laser beam is given on a fiber optic over an in-coupler. An external shutter which is driven by the controller of the camera provides that illumination takes place only during exposure. Thus, bleaching of the dye should be reduced. A loudspeaker running with suitable frequency and pulsform stimulates the mechanical natural frequency of the fiber optic. Hence, temporal mixing of the modes results, and speckles disappear nearly totally. By additional optics, in this case a liquid crystal fiber, the light is brought onto the sample. The sample lies on a heatable plate which can be adjusted in two directions. Beyond the probe table, the camera with the objectives and the filter are mounted. A controller connects the camera to the computer. The camera is movable in the z direction.

higher than the front velocity of any possible amplification wave. Each of these channels was etched only 20 μm wide and 10 μm deep yielding a flow rate inside the inlet channels about 20 times higher than in the reaction chamber. The volume of the complete reactor including inlets and outlets was about 2.5 μL. For faster filling, easier removal of air bubbles, and initialization of the reaction, two additional capillaries were connected laterally to the reaction chamber. These were closed during subsequent experimentation.

Generally, the high surface-to-volume ratio given in microstructures negatively affects the amplification of biochemical systems.[45] At the surface of the microreactor, some adsorption of the molecules (e.g., enzymes and nucleic acids) occurs. These molecules contribute only marginally if at all to the reaction. To counteract such adverse effects, a passivation of the surface[46] and/or modification of the reaction solution[47] is advisable. We tested several methods, such as coating with various silanes, to passivate the surface. In the experiments presented here, we used the following pretreatment. All reactors were treated for several hours with DEPC water (1 mL/L diethylpyrocarbonate/H_2O) to eliminate the enzymatic activity of ribonucleases. The DEPC was removed by flushing autoclaved DEPC water and autoclaved water through the reactor. To prevent adsorption at the surface of the reactor, the reactor was prefilled with a solution of BSA (free of nucleases) as above, dissolved in autoclaved water (0.4 μg/μL). In the experiments for the reaction waves, this final step was replaced by flushing a template free reaction solution through the reaction chamber for several minutes. A reaction solution with a template concentration in the range of 5−10 nM was pumped into the reaction chamber using the additional capillaries lateral to the reaction chamber (see Figure 1). After the solution was applied for about 20 min, the reactor was flushed with water until the detected fluorescence was again in the range of the dark signal. Finally, a template-free solution was pumped continuously through the reactor via the bifurcation structure.

2.3. Experimental Setup. The experimental setup is sketched in Figure 2. The microreactor, as described in the previous section, was maintained at constant reaction temperature (42 °C) on a copper plate by a temperature control loop. Syringe pumps (SP200 Series, World Precision Instruments, Inc.) were used to fill the reactor with the initial solution and to continuously feed the resource solution to it. A 1 mL syringe was employed in the syringe pump so as to have a flow rate tuneable over a wide range. A pump rate of 0.2 μL/min corresponds to a flow velocity of approximately 42 μm/min in the reaction chamber, calculated with a cross-sectional area of 60 mm × 80 μm perpendicular to the flow. The reaction solutions were kept in polyethylene tubes (as above) and cooled in an ice bath (in the dark).

The biochemical amplification in the reactor was monitored by detecting the intensity of emitted fluorescence. Excitation of TO-PRO-1 was induced by an argon ion laser (Spectra Physics, CA) at 488 nm. A digital camera (CCD camera CH250, Photometrics, AZ) cooled to −41 °C was used for detection, encompassing a CCD chip (KAF 1400, Kodak, Japan) with a size of 9 × 7 mm^2 and a resolution of 1317 × 1035 pixels. The camera has 4096 gray levels (=12 bit) and a full well capacity of about 40 000 electrons/image element. The reactor heating plate was placed on a stage which could be moved along two axes in the *xy* plane, and the camera height was also adjustable (*z* direction). Computer control of stepping motors via a pulse controller (Isel Automation, Eiterfeld, Germany) was used to position the camera and the reactor.

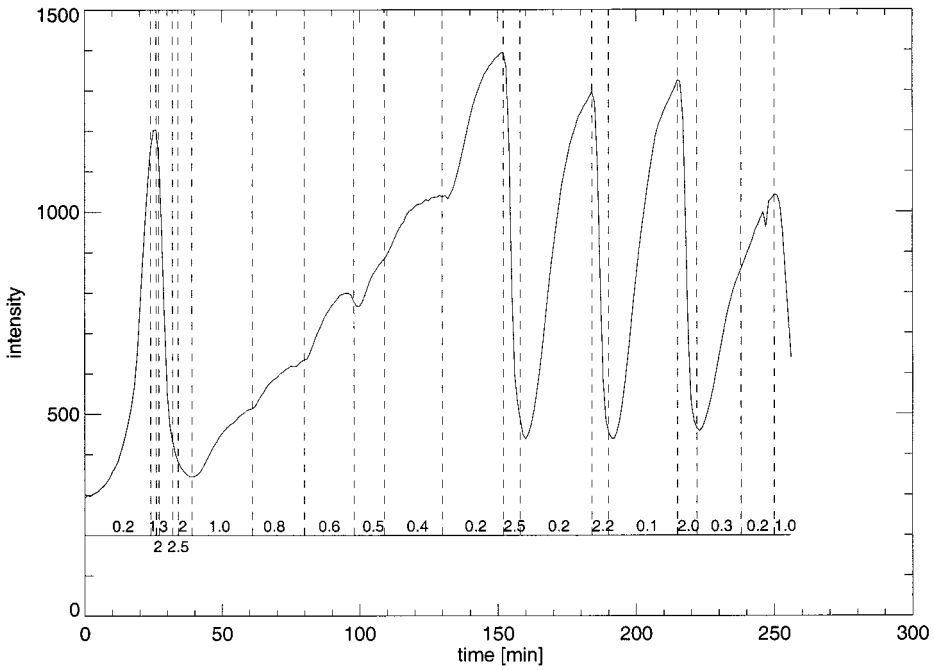

Figure 3. Fluorescence signal averaged over the reaction chamber versus reaction time. Regions of different flow rates are separated by dashed vertical lines; the numbers printed at the bottom of the lines represent the macroscopic pump rates in μL/min. The initial reaction solution with templates (5−10 nM) was pumped directly into the reaction chamber using the lateral inlet, bypassing the bifurcation structure. The lateral capillaries were then closed, and the amplification of double-stranded regions was detected using the fluorescent intercalating dye TO-PRO-1.[38] The light intensity on the probe was about 17.7 mW/cm^2 with an exposure time of 0.7 s.

The laser beam was focused into a multi-mode optical fiber (i.d.. 5.0 mm) after passing it through an external shutter. A TTL signal from the camera controller (AT200, Photometrics, AZ) opened the shutter only during image exposure. The response time of this external shutter was 50 ms. Interfering laser modes lead to a speckled illumination pattern. To rectify this, we acoustically modulated the fiber curvature (75 Hz).[48] Beam homogeneity was further improved by subsequent passage through a liquid crystal fiber (i.d., 2 mm). The optical angle of incidence was varied depending on the distance of the imaging objective (Zeiss Distagon T* 1:1.4, $f = 35$ mm) from the sample. The emission filter (Omega 545DF60, OMEGA Engineering, Inc., Connecticut) placed between the camera and the objectives had an optical density of 5 at 488 nm and transmission of 70−80% in the range of 520−570 nm. For data acquisition and initial image processing, the software PMIS, version 2.0.1 (Photometrics, AZ) was used. Additional analysis of the images was performed with IDL (version 5.0, IRIX mipseb, Research Systems, Inc.) and the authors' own code.

3. Results and Discussion

In contrast to the amplification of RNA in translucent polyethylene capillaries published in previous work,[17,18] the current experimental set up runs as an open system. The reactor is fed continuously with reaction solution and products are removed by the applied external flow. The pump rate determines the velocity of this feed and removal. However, the influence of the flow rate on the amplification system is not obvious and is strongly connected to the complex kinetics of the biochemical system. For an autocatalytic amplification

$$A \xrightarrow{k} 2A$$

as takes place for example in the initial phase of the 3SR reaction,[29] the flow rate would act as an effective death term (f). The death term f decreases the exponential growth rate of template (concentration a) from k to $k-f$

$$a(t) = a_0 \exp[(k - f)t]$$

The concentration of product increases for $f < k$, and for any flow rate above the critical flow rate $f_c = k$, the template concentration will be diluted out. The total rate of amplification or dilution results from an interplay between the exponential amplification of the biochemical system and a loss term produced by the flow. The system is able to commence from an arbitrarily small initial template concentration a_0.

In contrast, the amplification in a purely cooperatively coupled CATCH system is theoretically characterized at low concentration by hyperexponential growth.[33,49] As in the uncoupled 3SR reaction, a bifurcation analysis shows the existence of a critical flow rate above which the system will be diluted out. However, the trivial fixed point at zero template concentration is locally stable even for flow rates below the critical flow rate, and thus, the system can commence only for sufficiently large initial template concentrations. The tri-cyclic system applied in our experiments includes reaction steps for cooperative and non-cooperative amplification.

Our experimental results showed an amplification of the tri-cyclic system in the flow reactor for very low initial template concentrations (less than nM). Experiments done for comparison using the purely cooperative coupled system (CATCH) indicated that a cooperative amplification is not possible below a critical initial concentration (even for small flow rates). The influence of the flow rate on the amplification of the tri-cyclic system is demonstrated in Figure 3. In these experiments, the initial reaction solution with templates (5−10 nM) was pumped directly into the reaction chamber using the lateral inlet, bypassing the bifurcation structure. The lateral capillaries were then closed, and the amplification of double-stranded regions was detected using the fluorescent intercalating dye TO-PRO-

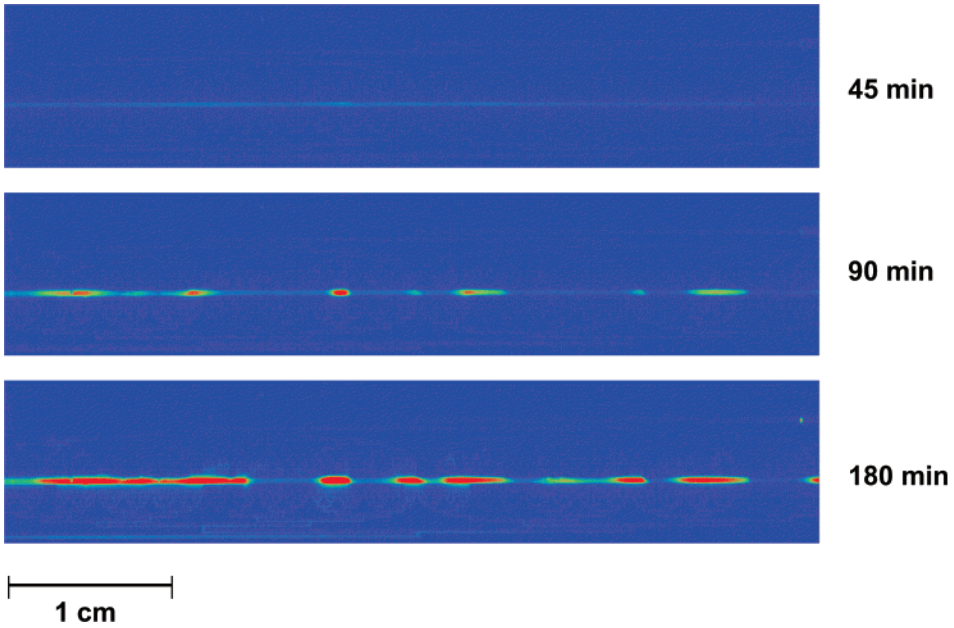

Figure 4. Three snapshots of the reactor showing inhomogeneous growth at different times in a long time experiment. Pseudocolor presentation is used for the image, with a rainbow color table. Red represents a high concentration region of double-stranded oligonucleotides. Black represents low concentrations. A reaction solution with templates (5−10 nM) was introduced into the reaction chamber using the lateral inlet. After obtaining a spatially homogeneous amplification for 30 min, the reaction chamber was flushed with autoclaved water (pump rate 4 μL/min) for about 20 min. The additional inlet and outlet were then pinched off. As the intensity of the detected signal reached the range of the original dark signal, a template-free reaction solution (solution I) was pumped at 2 μL/min through the bifurcation structure into the reactor. After 1 min, the pump velocity was reduced to 0.2 μL/min. Because the feed solution included no additional templates, amplification must then commence from polynucleotides left in the reaction chamber (by adsorption on the surface). Because no increasing signal was observed during the first 67 min of this experiment, the pump rate was increased to 2 μL/min for 1 min and then reduced again to 0.2 μL/min for the rest of the experiment. After this procedure, the fluorescence signal started to increase, indicating a rise in the concentration of double stranded polynucletides in the reaction chamber. The capacity of light on the sample was 17.7 mW/cm^2. The exposure time was 1 s. The resolution is about 38 μm/pixel.

1.[38] When the fluorescence signal indicated sufficient amplification of the templates, the experiment was started by pumping template-free reaction solution into the chamber using the bifurcation structure. We alternated between high and low pump rates to show the feature of the flow rate control of amplification. For slow pump rates, the concentration of polynucleotides rose, whereas for high pump rates, the products were diluted out. This result demonstrates both the existence of a critical flow rate and a complete renewal of the entire reaction products in the microfluidic device is feasible.

No evidence was found for the existence of a critical minimal initial concentration. This supports an initial exponential amplification by an RNA-Z like mechanism. This was also circumstantiated by the shape of the intensity curve shown in Figure 3. The averaged emitted fluorescence intensity can be approximated in the initial phases of growth or dilution by an exponential curve. A fit (nonlinear χ^2-approximation with the Marquardt−Levenberg algorithm) for various flow rates yielded an exponential rate of $k = 0.27 \pm 0.07$ min^{-1} which corresponds to a doubling time of 154 s and an extrapolated critical flow rate of 0.85 $\pm$ 0.3 μL/min. This exponential rate for the amplification inside the microfluidic device was slower than the initial growth rates of the tri-cyclic system obtained in standard fluorimeter experiments with no flux; a doubling time of about 35 s was measured in the latter experiments.[37,50] The comparably slow amplification inside the reactor is most likely a result of surface adsorption effects.

Simple exponential amplification does not yield any complex pattern formation, and indeed, the emitted light intensity observed during the initial reaction period was rather homogeneous. Complex pattern formation on the other hand would be necessary to stabilize cooperative molecular functionality in evolutionary flow experiments.[13]

Spontaneously growing spots were observed in long time experiments under small flow rates. A particular example of such an inhomogeneous growth is shown in Figures 4 and 5. Three different phases were typically observed in these experiments. The reaction started with (exponential) homogeneous growth which merged into a transient phase of constant concentration in the entire reaction chamber (Figure 6). Experiments under identical conditions but omitting one of the nucleotides (UTP) necessary for growth confirmed the amplification origin of this signal. After this transient time phase, further growth started locally by self-ignition in several places, randomly over the length of the reactor. From these reaction seeds, spots of high concentration grew by propagating reaction−diffusion distributed fronts with a rather steep and exponentially decaying shape. New spots emerged during the whole observation time. Contour lines were computed at intensity values $I = 1200$ cps $+ n \times 100$ cps, $n = 1, 2, ...,$ 26 and time greater than 200 min for five spots which could be well distinguished from other spots during the course of the experiment. Tangents to these contour lines yield front velocities. Whereas the velocities of the fronts propagating to the right were not significantly different from zero, the velocities of the left fronts were between 0.17 and 0.32 μm/s, with an average value of 0.261 μm/s. Counterbalancing the left-right asymmetry gives an effective front velocity of about 0.131 μm/s. A natural barrier for the diffusion and the propagation of wave fronts in such experiments were air bubbles in the reaction chamber. In this experiment, such a stationary bubble was placed at $x \approx 0.5$ cm (130 pixels). It was first observed as a small stripe and later as a sharp border between different reaction waves. At $t \approx 250$ min the bubble became unstable in the flow and disturbed the surrounding pattern produced by the reaction waves.

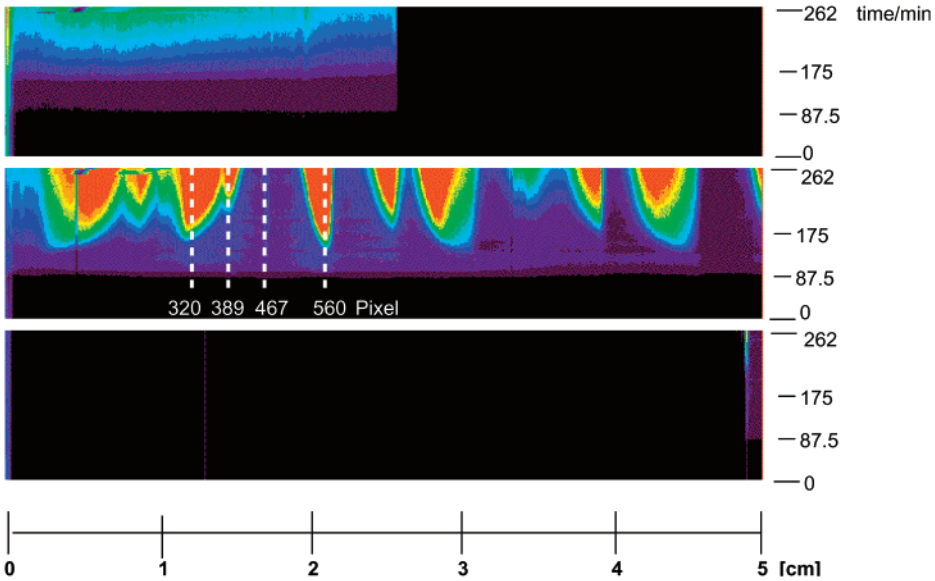

Figure 5. Space-time development of light intensity in the outlet channel (upper part), the reaction chamber (middle part), and inlet channel (lower part) for the experiment shown in Figure 4. The time row was obtained by averaging the signal from the reaction chamber in flow direction, at constant time intervals of one minute. A pseudocolor presentation was used as in Figure 4. The influx was monitored in a channel parallel to the reactor coming from the right to the middle of the reactor, and the outflux was monitored in a channel from the middle of the reactor going to the left. No signal was detected in the inflow channel, indicating an absence of polynucleotide production in the inlet structure. In the reaction chamber (middle image), an inhomogeneous growth of polynucleotides was observed.

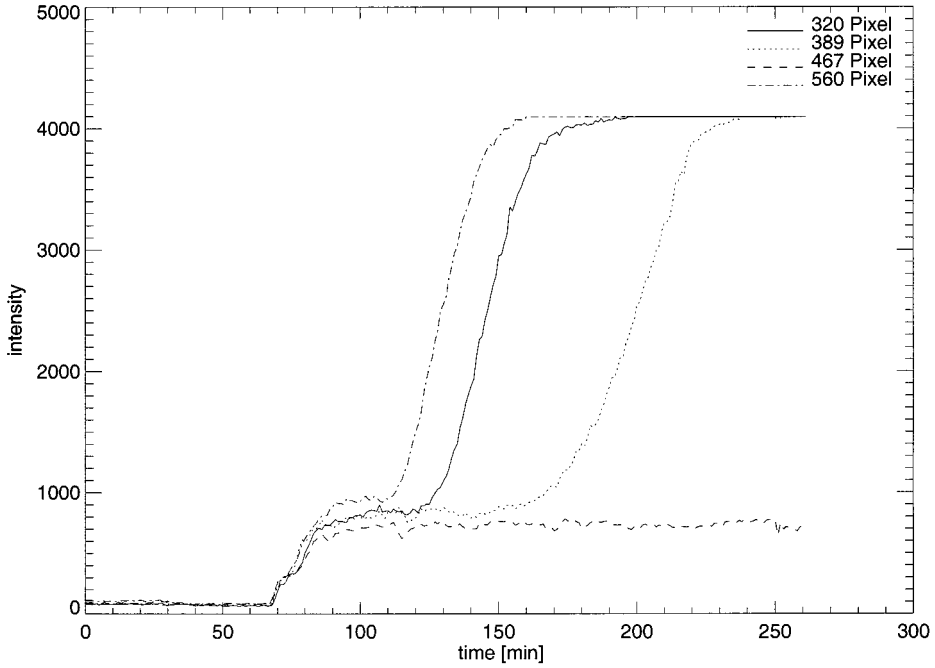

Figure 6. Intensity versus time at various space points in the reactor for the space-time development in Figure 5. The growth is plotted for the space points $x_1 = 320$ pixels ($\approx$1.2 cm), $x_2 = 389$ pixels ($\approx$1.48 cm), $x_3 = 467$ pixels ($\approx$1.77 cm), and $x_4 = 560$ pixels ($\approx$2.13 cm), respectively. The spatial points x_1, x_2, and x_4 lie in regions of further amplification, whereas x_3 lies in a region between two spots. At all these points, the intensity grew during 20 min (from 67−90 min) and then stabilized to values between 700 and 1000 cps. Although the intensity at x_3 then remained constant at this value (excepting minor fluctuations), the intensity at the other three points started to increase at different time intervals and reached the full well capacity value (4096 cps) of the CCD camera.

To investigate the source of this secondary amplification, we must consider the experimental homogeneous growth kinetics of the tri-cyclic system. This was studied using fluorescence detection with TO-PRO-1 in a thermostated fluorimeter.[50] In these experiments, the system reaches an intermediate plateau at relatively high concentration followed by a secondary phase of growth. A transient phase and nonhomogeneous growth have also been measured in experiments with the tri-cyclic system in translucent polyethylene capillaries without any flow (unpublished results). In comparison to these batch experiments, the intermediate plateau in flow experiments occurred located at low concentrations ($\approx 10^{-8}$−10^{-9} M) relative to the final saturation ($\approx 10^{-6}$ M).

The fact that further growth is possible following the intermediate plateau in the tri-cyclic system indicates that this plateau is not a result of resource depletion or generic product inhibition (e.g., by pyrophosphate) but is caused by a specific self-inhibition of the RNA-Z species. Such self-inhibition of

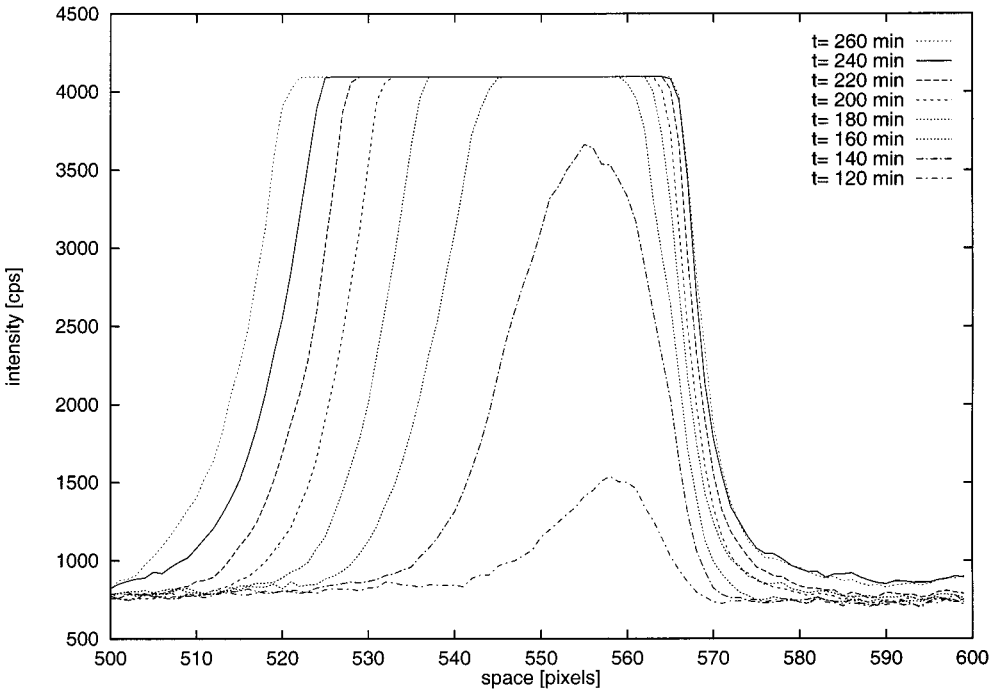

Figure 7. Intensity versus space at various time points. Plotted is the space region from 500 to 600 pixels, at which a single spot emerged. The spot has a steeper right than left front. Theoretical simulation showed that a slight flow perpendicular to the inlet flow direction, together with adsorption effects to the surface of the reaction chamber, can result in such an asymmetric profile. The wave front stabilized for $t \geq 180$ min to a rather steep and exponentially decaying shape ($f(x) = I_0 \exp^{-\gamma x}$). The left−right asymmetry, however, makes it difficult to determine a wave front velocity.

growth can take place both through RNA−DNA and DNA−DNA hairpin interactions, leading to complexes which are inactive for transcription. Such an intermolecular side reaction would restrict the RNA-Z amplification to concentrations below the binding constant of the intermolecular loop interaction. Gel analysis of the products of the tri-cyclic reaction indicate that all of the reaction intermediates for the coupled amplification mechanism are present at higher concentrations, verifying the tri-cyclic mechanism of growth in the secondary growth phase.[37]

We are now in a position to explain the origin of inhomogeneous waves in the system, despite the fact that template levels are much higher than necessary for local waves to originate as single template clones. The coupled kinetics of the cross-catalytic part of the tri-cyclic mechanism, like the CATCH system itself, has a greater than linear template concentration dependence. At low concentrations u, the cooperative CATCH mechanism has been shown to give rise to amplification proportional to $f(u) = u^{3/2}$,[33] and this behavior is expected for the onset of the secondary growth phase (albeit masked by saturation effects of the RNA-Z mechanism in the experiments). In contrast with exponential amplification, which can start at arbitrarily low concentrations in a flow reactor (see above), higher order amplification requires a minimum threshold concentration for growth to overcome the dilution outflow. The most thoroughly studied theoretical kinetic models for spatial amplification waves are the logistically constrained growth law $f(u) = u(1 - u)$ studied by Fisher[51] and the cubic form $f(u) = u^2(1 - u)$ studied in the theory of flame propagation.[52] Although the Fisher equation shows linear dependence at low concentrations leading to exponential growth (often called quadratic growth in the reaction−diffusion literature reflecting the overall polynomial structure), the latter model has a quadratic dependence at low concentration like the hypercycle equations.[5] In terms of theoretical models,[52] the noncooperative mechanism corresponds to a quadratic autocatalyst, whereas the cooperative amplification mechanism corresponds to a cubic one. Quadratic and cubic autocatalysis are both able to produce propagating reaction−diffusion fronts, which migrate with steady velocity and constant, exponentially decaying waveform. For the speed of a wave front c produced by the quadratic amplification with growth rate k and diffusion constant D, the well-known Fisher formula $c = 2(kD)^{1/2}$ can be applied. A similar expression exists for the cubic form above with a slower speed of propagation $c = (kD/2)^{1/2}$.[53,52] For the $f(u) = u^{3/2}(1 - u)$ case, more accurately reflecting the overall kinetics of the cooperative mechanism, an intermediate front velocity is expected. In the case of nonzero flow, the higher order autocatalytic waves must be triggered by a sufficiently large initial concentration (u^*) of templates. An analogous quenching phenomenon is known for the ignition of flame propagation.[52] In the case of exponential growth, a necessary condition for wave fronts to arise is a localized initial concentration of templates, a condition not met in our flow experiments. On the other hand, a higher order autocatalyst, such as in the cooperative amplification mechanism above, is unstable to local perturbations induced by local concentration fluctuations. This is the origin of self-replicating spot patterns in the resource limited $2A \rightarrow 3A$ reaction (Scott Gray mechanism).[54] Such behavior could account for the pattern formation observed in the later phase of the flow experiments. During the transient phase separating the spatially homogeneous growth from the initiation of amplification waves, the concentration of polynucleotides u was not sufficiently high to stimulate cooperative amplification immediately. In this state, the system is excitable and unstable to local perturbations which can stimulate reaction−diffusion fronts. A surprising result was the rather asymmetric growth of the spots (Figures 5 and 7), because we were not able to detect any asymmetry in the flow system using fluorescent beads. Numerical simulation (not presented here) showed that a small component (10%) of the flow along the effective one-dimensional open reactor, combined with

partial immobilization of products on the surfaces, can lead to such asymmetric profiles. The left−right asymmetry makes it difficult to measure wave front velocities precisely in the experiments, but if we counterbalance the left−right asymmetry in Figure 5, we obtain an effective front velocity of 0.13 μm/s. Online flow control will be introduced in future experiments to improve this situation.

4. Conclusions

In summary, we have shown the first experiments on spatially resolved amplification in vitro in an open one-dimensional medium, allowing indefinite amplification. The results indicate not only that amplification and amplification waves can be studied in such a reaction setting but that novel cooperative amplification mechanisms with higher order concentration dependence can give rise to spatial patterns starting from homogeneous initial conditions in such spatially resolved flow reactors. We expect this type of experiment to become increasingly useful in the future, helping to provide an experimental base for evolutionary ecology using kinetically well-characterized molecular systems.

Acknowledgment. The experimental work was performed at the Institute of Molecular Biotechnology in Jena, Germany and was supported by grants from the German Ministry of Education, Science and Technology (BMBF, Grant No. 0310799). We thank Ralf Ehricht, Thomas Ellinger, Harald Mathis, Reiner Bräutigam, Kristina Schmidt, Marlies Gohlke, Arne Bochmann, Petra Foerster, Annette Wagenhaus, and Angelika Heller for technical support and discussions.

References and Notes

(1) Eigen, M.; McCaskill, J. S.; Schuster, P. *Adv. Chem. Phys.* **1989**, *75*, 149.
(2) Eigen, M. *Die Naturwissenschaften* **1971**, *58*, 465.
(3) Kauffman, S. A. *J. Cybernetics* **1971**, *13*, 71.
(4) Rössler, O. E. *Z. Naturforsch.* **1971**, *26b*, 741.
(5) Eigen, M.; Schuster, P. *Die Naturwissenschaften* **1977**, *64*, 541.
(6) Eigen, M.; Schuster, P. *Die Naturwissenschaften* **1978**, *65*, 7.
(7) Eigen, M.; Schuster, P. *Die Naturwissenschaften* **1978**, *65*, 341.
(8) Eigen, M.; Schuster, P. *The Hypercycle*; Springer: Berlin, 1979.
(9) Smith, J. Maynard *Nature* **1979**, *280*, 445.
(10) Bresch, C.; Niesert, U.; Harnasch, D. *J. Theor. Biol.* **1980**, *85*, 399.
(11) Dyson, F. J. *J. Mol. Evol.* **1982**, *118*, 344.
(12) Boerlijst, M. C.; Hogeweg, P. *Physica D* **1991**, *48*, 17.
(13) McCaskill, J. S. In Ursprünge der Molekularen Kooperation: Theorie und Experiment; *Antrittsvorlesungen 1994 an der Friedrich-Schiller-Universität Jena*; Schuster, P., Ed.; Institut für Molekulare Biotechnologie e. V.: Jena, Germany, 1995; p 27.
(14) Böddeker, B. *Physikalische Modelle für Koevolution und Simulation auf einem hardwareprogrammierbaren Prozessor*, Diploma Thesis, Universität Göttingen, Germany, 1995.
(15) McCaskill, J. S.; Maeke, T.; Gemm, U.; Schulte, L.; Tangen, U. *Lect. Note. Comput. Sci. 1259*; Springer-Verlag: New York, 1997; p 260.
(16) Cronhjort, M. B.; Blomberg, C. *Physica D* **1997**, *101*, 289.
(17) Bauer, G. J.; McCaskill, J. S.; Otten, H. *Proc. Natl. Acad. Sci. U.S.A.* **1989**, *86*, 7937.
(18) McCaskill, J. S.; Bauer, G. J. *Proc. Natl. Acad. Sci. U.S.A.* **1993**, *90*, 4191.
(19) Tam, W. Y.; Horsthemke, W. J.; Noszticzius, Z.; Swinney, H. L. *J. Chem. Phys.* **1988**, *88*, 3395.
(20) Ehrfeld, W.; Hessel, V.; Löwe, H. *Microreactors, New Technology for Modern Chemistry*; Wiley−VCH: Weinheim, Germany, 2000.
(21) Harrison, D. J., van den Berg, A., Eds.; *Micro Total Analysis Systems '98, Proceedings of the μTAS '98 Workshop*; Kluwer Academic Publishers: Dordrecht, The Netherlands, 2000.
(22) Wright, S. *Proc. VI Int. Congr. Genet.* **1932**, *1*, 356.
(23) Wright, S. *Ecology* **1945**, *26*, 415.
(24) Kimura, M. *Proc. Natl. Acad. Sci. U.S.A.* **1983**, *80*, 6317.
(25) Aoki, K. *J. Math. Biol.* **1998**, *25*, 453.
(26) Szathmáry, E. *Trends Ecol. Evol.* **1989**, *4*, 200.
(27) Ehricht, R.; Ellinger, T.; McCaskill, J. S. *Eur. J. Biochem.* **1997**, *243*, 358.
(28) Kwoh, D. Y.; Davis, G. R.; Whitefield, K. M.; Chappelle, H. L.; DiMichele, L. J.; Gingeras, T. R. *Proc. Natl. Acad. Sci.* **1989**, *86*, 1173.
(29) Guatelli, J. C.; Whitefield, K. M.; Kwoh, D. Y.; Barringer, K. J.; Richman, D. D.; Gingeras, T. R. *Proc. Natl. Acad. Sci.* **1990**, *87*, 1874.
(30) Fahy, E.; Kwoh, D. Y.; Gingeras, T. R. *PCR Methods Applications* **1991**, *1*, 25.
(31) Compton, J. *Nature* **1991**, *350*, 91.
(32) Romano, J. W.; Shurtliff, R. N.; Sarngadharan, M. G.; Pal, R. *J. Virol. Methods* **1995**, *54*, 109.
(33) Kirner, T.; Ackermann, J.; Ehricht, R.; McCaskill, J. S. *Biophys. Chem.* **1999**, *79*, 163.
(34) Ellinger, T.; Ehricht, R.; McCaskill, J. S. *Chem. Biol.* **1998**, *5*, 729.
(35) Breaker, R. R.; Joyce, G. F. *Proc. Natl. Acad. Sci. U.S.A.* **1994**, *91*, 6093.
(36) Breaker, R. R.; Banjeri, A.; Joyce, G. F. *Biochemistry* **1994**, *33*, 11980.
(37) Ehricht, R.; Design, Verwirklichung und funktional−evolutive Charakterisierung gekoppelter Amplifikation in vitro, Ph.D. Thesis, Friedrich-Schiller-Universität, Jena, Germany, 1998.
(38) Haugland, R. P. *Handbook of fluorescent probes and research chemicals*, 5th ed.; Molecular Probes, Inc.: Eugene, OR, 1992; p 223.
(39) Le Grice, S. F. L.; Cameron, G. E.; Binkovic, S. J. *Methods Enzymol.* **1995**, *262*, 130.
(40) Ellinger, T.; Ehricht, R. *BioTechniques* **1997**, *24*, 718.
(41) Schmidt, K.; McCaskill, J. S. In *Open Flow Microreactors*, Annual Report; Gumpert, J., Ed.; Institute of Molecular Biotechnology: Jena, Germany, 1996; p 92 (http://www.imb-jena.de/ANN_REP.html).
(42) McCaskill, J. S. *Biophys. Chem.* **1997**, *66*, 145.
(43) Schmidt, K.; Foerster, P.; Bochmann, A.; McCaskill, J. S. A microflow reactor for two-dimensional investigations of in vitro amplification systems. In *Microreaction Technology, Proceedings of the First International Conference on Microreaction Technology*; Ehrenfeld, W., Ed.; Springer: Berlin, 1998; p 234.
(44) Bräutigam, R.; Steen, D.; Ehricht, R.; McCaskill, J. S. Isothermal Biochemical Amplification in Miniaturized Reactors with integrated Micro Valves. *Microreaction Technology, Proceedings of the third International Conference on Microreaction Technology*, Frankfurt a. M.; Springer: Berlin, 1999, in press.
(45) Hlady, V.; Buijs, J. *Curr. Opin. Biotech.* **1996**, *7*, 72.
(46) Schoffner, M. A.; Cheng, J.; Hvichia, G. E.; Kricka, L. J.; Wilding, P. *Nucl. Acids Res.* **1996**, *24*, 375.
(47) Taylor, T. B.; Winn−Denn, E. S.; Picozza, E.; Woudenberg, T. M.; Albin, M. *Nucl. Acids Res.* **1997**, *25*, 3164.
(48) Dapprich, J. *Fluoreszenzdetektion molekularer Evolution*; Georg-August-Universität: Göttingen, Germany, 1994.
(49) Kirner, T.; Ackermann, J.; Steen, D.; Ehricht, R.; Ellinger, T.; Foerster, P.; McCaskill, J. S. *Chem. Eng. Sci.* **2000**, *55*, 245.
(50) Kirner, T. *Musterbildung in biochemischen in vitro Amplifikationssystemen*, Ph.D. Thesis, Friedrich-Schiller-Universität, Jena, Germany, 2000.
(51) Fisher, R. A. *Ann. Eugenics* **1937**, *7*, 355.
(52) Sott, S. K.; Showalter, K. *J. Phys. Chem.* **1992**, *96*, 8702.
(53) Voronkov, V. G.; Semonov, N. N. *Zh. Fiz. Khim.* **1939**, *13*, 1695.
(54) Pearson, J. E. *Science* **1993**, *261*, 189.